ACS ES&T Engineering

pubs.acs.org/estengg

Article

# Technical and Cost Assessment of Electrocatalytic Bromate Removal from Drinking Water

Kuan-Lin Lee, Chenxu Yan, Jingwen Xu, Carolyn E. Brady, and Charles J. Werth*

Cite This: *ACS EST Engg.* 2024, 4, 2186–2197

Read Online

ACCESS | Metrics & More | Article Recommendations | Supporting Information

**ABSTRACT:** Bromate is a potential human carcinogen and is commonly found in water and wastewater after ozonation. Electrocatalytically, Pd has shown good activity in reducing bromate to bromide; however, the energy efficiency and cost of this technology in a realistic treatment system remain unknown. A custom filter-press reactor with minimal mass-transfer limitations was used to test the kinetics and energy consumption for bromate reduction using Pd, Ru, or Cu on activated carbon cloth as the cathode. In phosphate-buffered nanopure water at circumneutral pH, 95% of bromate was reduced to bromide (from 200 to 10 $\mu$g/L) in 1 h with a normalized activity of 2136 mL min$^{-1}$ $g_{Pd}^{-1}$. The total energy consumption was 0.576 kW h per gram of bromate removed, which is 9 to 43 times lower than that in reported studies. In Austin tap water (TW) at pH 9.5, the normalized activity dropped to 544 mL min$^{-1}$ $g_{Pd}^{-1}$, and the total energy consumption increased to 2.198 kW h per gram of bromate removed, still an improvement over all values reported in the literature despite the latter using synthetic waters. This superior performance is due to the design of the filter-press reactor that minimizes mass-transfer limitations as well as solution resistance compared to reactors evaluated in the literature, such as batch and three-dimensional electrochemical reactors. We note that any lost activity due to catalyst oxidation and poisonings in TW can be electrochemically regenerated by briefly applying a positive and strongly negative potential. This electrocatalytic treatment has estimated costs of $1.41 per 1000 gal (91% capital costs and 9% O&M costs) and is comparable to ion exchange, granular activated carbon, and reverse osmosis, yet benefits from no waste stream generation, indicating that this technology is ready for evaluation at the pilot scale.

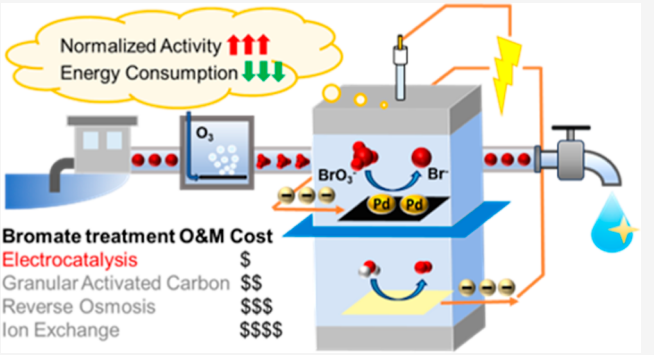


**KEYWORDS:** *electrocatalytic reduction, bromate, palladium, cathode regeneration, cost assessment*



## 1. INTRODUCTION

The process of ozonation to disinfect drinking and wastewater produces bromate ($BrO_3^-$) as a byproduct,[1,2] which results in elevated concentrations of bromate in the environment and drinking water. Due to human health concerns, the International Agency for Research on Cancer (IARC) classified bromate as a potential carcinogen, and the U.S. Environmental Protection Agency regulates bromate at a maximum contaminant level (MCL) of 10 $\mu$g/L. Bromate treatment options are limited, expensive, and only marginally effective.[3] This is a concern because more ozone use is anticipated to remove micropollutants from drinking water and from wastewater being treated for potable reuse, especially in light of increasing levels of bromide ($Br^-$) in natural waters due to anthropogenic inputs.[4] This concern motivates the need to develop a more robust and inexpensive treatment option for bromate.

Conventional technologies considered for bromate treatment include ion exchange (IX), granular activated carbon adsorption (GAC), reverse osmosis (RO), and various chemical reduction strategies.[1,5−7] Both IX and RO create secondary waste streams that contain concentrated bromate and/or salt, which limits the application of these technologies to locations where inexpensive waste disposal is available.[8] Further, RO operates at high pressures with energy demands that are prohibitively expensive unless concomitant salt removal is required. GAC has only moderate adsorption affinity for bromate, and the bromate-laden GAC still requires regeneration or disposal; these factors make this technology expensive as well as unsustainable. Last, chemical reduction (e.g., $Fe^0$) suffers from poor removal efficiency and high costs at low but regulated bromate levels, leaving no favorable economical options for treating this problematic pollutant.

Received: April 14, 2024
Revised: July 23, 2024
Accepted: July 24, 2024
Published: August 5, 2024

Catalytic and electrocatalytic treatments have emerged as promising options for bromate treatment. Both convert bromate to relatively harmless bromide, and there are no problematic byproducts.[9,10] However, catalytic treatment requires the addition of hydrogen gas as the electron donor, and there are concerns regarding the safety of handling and storing hydrogen gas. Additional concerns include catalyst deactivation with lack of a facile regeneration method and associated cost uncertainties.[11,12] Electrocatalytic reduction appears more promising, as an electric current and not hydrogen gas is used to drive the bromate reduction reaction (BRR). As with catalytic treatment, electrocatalytic deactivation is expected with prolonged treatment,[13] but when similar systems are investigated, there is promise that a temporary strongly positive or negative potential can be applied in situ to regain catalyst activity.[14,15]

Many electrocatalytic studies have been performed in batch systems, where fluids are well mixed and both reaction kinetics and Faradaic efficiency (FE) are determined.[16−18] Reaction kinetics and FE depend on a variety of factors, most importantly, electrode material and the aqueous chemistry of the system. The most common cathodes are platinum group metal (PGM) nanoparticle catalysts (e.g., Pd, Pt, and Ru) loaded onto conductive carbon supports such as glassy carbon and carbon fiber paper. Other metals used are bimetallic catalysts that alloy a PGM with a nonprecious metal,[19] coinage metal catalysts (primarily copper, Cu), or zerovalent iron (ZVI).[16,20,21] PGM-based cathodes generally show the highest activity per mass of metal, while Cu often shows the most activity per cost of metal. However, Cu is subject to significant leaching,[22] and ZVI is a reductant that depletes over time. The effects of water chemistry are complex, and for typical drinking water conditions the most challenging constituents are those that promote catalyst deactivation over time, including poisons like reduced sulfur species (e.g., $S^{2-}$),[23−25] and surface foulants like natural organic matter (NOM).[26] Catalyst deactivation has also been attributed to excess metal surface oxidation that may occur during pollutant reduction.

Very few studies have evaluated electrocatalytic bromate reduction in continuous flow reactors that more accurately represent electrochemical systems used in related industrial processes such as chloralkali production. A common design for continuous flow is the parallel-plate reactor, which is typically limited by mass transfer of reactant(s) to the electrode surface resulting in markedly slower reaction rates than in batch.[27] An alternative design is the parallel-plate, thin-layer (PPTL) electrochemical flow reactor, also known as the filter press reactor,[28] which was recently shown to practically eliminate mass-transfer limitations for aqueous nitrite reduction at the cathode surface.[15] A key concern for those in the industry is whether the power needed for PPTL flow reactors is more expensive compared with conventional technologies. This is directly related to the applied potential and associated current needed for bromate reduction.[29] Power requirements have been reported in a limited number of studies but generally without comparison to other electrocatalytic studies and not in terms of costs relative to conventional technologies (e.g., RO, IX, GAC). As a result, it is not clear whether electrocatalytic bromate treatment is ready for pilot-scale testing and assessment.

The goal of this work is to evaluate the technical and financial feasibility of electrocatalysis (EC) for the removal of bromate from drinking water. We address the hypothesis that bromate can be treated in a PPTL flow reactor at a material and energy cost that is small compared to the capital and operating expenses of conventional bromate treatment technologies. We test this hypothesis by first identifying the applied potential and catalyst metal that maximize the bromate reduction activity and minimize the competing hydrogen evolution reaction (HER). Next, we use the optimal catalyst metal and applied potential, measure bromate reduction kinetics, FE, and overall applied potential in phosphate-buffered nanopure water (PW) and tap water (TW), and estimate the overall power requirements. We also evaluate catalyst deactivation over time and test in situ regeneration of catalyst activity using a positive and strongly negative applied potential. The material and energy costs are then compared to several competing technologies to assess whether electrochemical bromate reduction holds promise for larger scale evaluation.

## 2. METHODS

**2.1. Chemical Reagents.** $Pd(NO_3)_2{\cdot}2H_2O$ (~40% Pd basis; Sigma-Aldrich), $Cu(NO_3)_2{\cdot}2H_2O$, and $Ru(NO_3)_2{\cdot}2H_2O$ were used to prepare catalyst precursors for Pd, Cu, and Ru catalyst deposition onto a carbon support electrode. Pd, Cu, and Ru were chosen because their use is widely reported in the literature for bromate, nitrite, and nitrate reduction.[15,19,30] Activated carbon cloth (ACC) from Gun EI Chemical Industry (Japan) served as the carbon support; published physical and chemical properties are presented in Table S1. ACC was chosen because when decorated with Pd, high activity for nitrite reduction was observed.[15] $KBrO_3$ (99.8%, Alfa Aesar) was the bromate source. $KH_2PO_4$ (99%; Sigma-Aldrich) and $K_2HPO_4$ (98%; Sigma-Aldrich) were used to prepare 0.02 M buffer solution, which served as both an electrolyte and buffer solution (pH 6.5 ± 0.1). TW was obtained from the University of Texas at Austin campus and is sourced from Austin Water. Major TW constituents are presented in Table S2. $HNO_3$ (70%, TraceMetal grade, Fisher Scientific) was used for digestion to separate the catalyst metals from the carbon supports. $K_2SO_4$ (99%; Sigma-Aldrich) was used as an electrolyte to increase the ionic strength. $H_2SO_4$ (95−98%; Sigma-Aldrich) was used to adjust the pH in solutions. All solutions were prepared in nanopure water (18.2 MΩ·cm) produced by a Barnstead Nanopure system (Thermo Fisher Scientific).

**2.2. Cathode Preparation.** The ACC was cut into 2.0 × 2.5 $cm^2$ pieces (0.12 ± 0.01 g). Different metal catalyst (Me) precursor solutions, $Pd(NO_3)_2{\cdot}2H_2O$, $Ru(NO_3)_2{\cdot}2H_2O$, or $Cu(NO_3)_2{\cdot}2H_2O$ solutions, were separately drop-casted onto separate ACC pieces using incipient wetness impregnation.[31−33] The method is described in Supporting Information in detail.

**2.3. Bromate Reduction Experiments.** A three-electrode PPTL flow reactor from Yan's work was used for bromate reduction experiments.[15] A schematic is shown in Figure S1. Three electrodes are the aforementioned Me/ACC cathode, an $IrO_2$ anode for efficient oxygen evolution reaction,[34] and a commercial reference electrode (Ag/AgCl, CH Instruments), herein referred as RE, for control the applied potential. Details of the PPTL flow reactor are included in Supporting Information.

Two 40 mL vials serve as reservoirs for the cathodic and anodic feed solutions. The former contains bromate in either the 0.02 M phosphate-buffered nanopure water (PW)


https://doi.org/10.1021/acsestengg.4c00203
ACS EST Engg. 2024, 4, 2186−2197

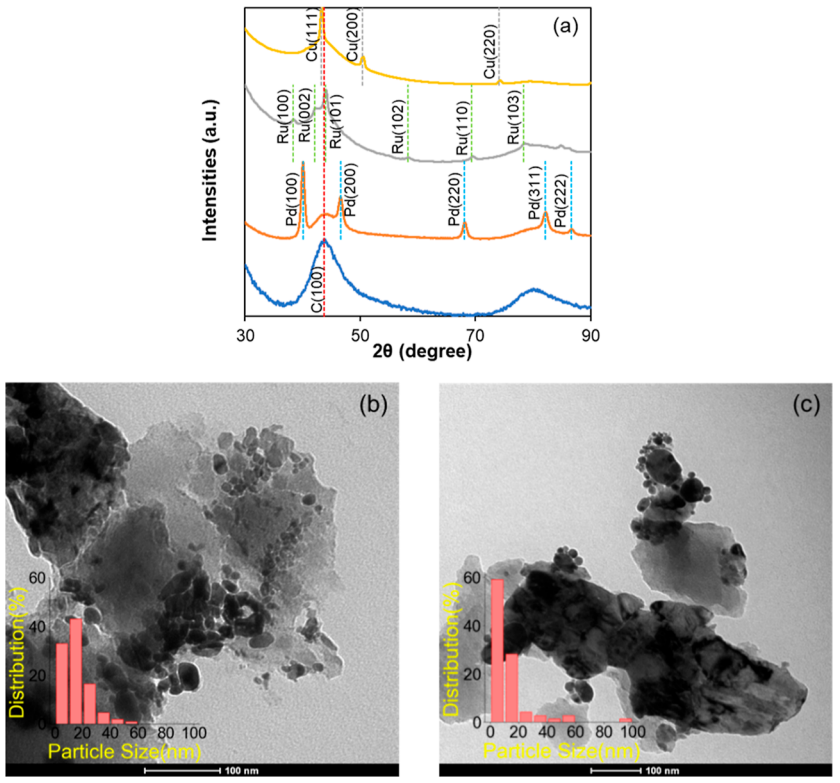


**Figure 1.** (a) PXRD patterns of ACC, Pd/ACC, Ru/ACC, and Cu/ACC. The dashed lines represent locations of characteristic peaks of C, Pd, Ru, and Cu. (b) Low-resolution TEM image of catalyst metal particles in unused Pd/ACC and (c) used and regenerated Pd/ACC.

($KH_2PO_4$, $K_2HPO_4$, pH: 6.5 ± 0.1), TW, or modified TW, while the latter contains the same solutions without bromate. During bromate reduction experiments, both reservoirs were rapidly mixed using a magnetic stir bar and continuously pumped in recirculation mode through their respective chambers at 40 mL/min using a peristaltic pump (Masterflex). This flow rate was previously shown to minimize mass-transfer limitations relative to reaction limitations in the PPTL flow reactor.[15] A potentiostat (Gamry 1010E) was connected to the working (i.e., cathode), counter (i.e., anode), and reference electrodes to control the applied potential and supply current. The applied potentials for all experiments were corrected for the uncompensated solution resistance between the working and reference electrodes by using the current-Interfere *iR* compensation technique supported by the potentiostat. All bromate reduction experiments were performed in triplicate.

Multistep chronoamperometry was used to determine the applied potential that maximized BRR and minimized HER for each working electrode, i.e., Pd/ACC, Ru/ACC, and Cu/ACC. The potential was stepped in −0.1 V increments from 0.0 to −0.9, −0.8, and −1.1 V/RE for Pd/ACC, Ru/ACC, and Cu/ACC, respectively. Each cathode was tested with two sets of multistep CA experiments. The experiment was first done with no bromate addition in the reservoir and then an initial bromate concentration of 1000 mg/L was added into the cathodic reservoir. The current over time at each potential step was recorded with the potentiostat.

The CA technique was used to test the kinetics of bromate reduction with three different working electrodes. The initial bromate concentration of each experiment was 200 $\mu$g/L, 1, or 12.79 mg/L. Bromate reduction was monitored for 1 h. The lowest concentration mimics problematic bromate concentrations found in drinking water after ozone treatment. The two higher concentrations were selected to explore the impact on FE. The applied potential was determined from multistep CA experiments and was −0.6, −0.6, and −0.7 V/RE for Pd/ACC, Ru/ACC, and Cu/ACC, respectively. Aqueous samples were taken at selected time points from the cathodic reservoir during each experiment and analyzed by ion chromatography (IC) for $Br^-$ and $BrO_3^-$. The pH was monitored at the beginning and end of each experiment and was relatively constant with the added phosphate buffer.

**2.4. Analytical Methods.** Aqueous samples containing bromate and bromide were analyzed by IC (Thermo ICS-2100) using a Dionex IonPac AS19 column and a 250 $\mu$L sample loop. The eluent was 12.5−45 mM KOH, and the flow rate was 1 min/L. Catalyst metal loadings on ACC were analyzed by inductively coupled plasma-optical emission spectroscopy (ICP-OES, Agilent 5800 ICP-OES coupled with SPS 4 autosampler) after cutting each electrode into small pieces, digesting one or more pieces in a 70% $HNO_3$ solution for 2 days at room temperature, filtering the digest, and then diluting the concentrated filtrate with nanopure water 35 times into 2% $HNO_3$ solution. The crystal structure of catalyst metals on ACC was measured using powder X-ray diffraction (PXRD, Rigaku R-axis Spider diffractometer) with a Cu source, operated at 40 kV and 40 mA. Catalyst metal nanoparticle sizes were determined from images obtained using a low-resolution transmission electron microscope (FEI Tecnai TEM) operated at 80 kV, and TEM images were processed by ImageJ software. TEM samples were prepared by grinding electrode pieces into a powder, dispersing the powder in ethanol, and then drop-casting on a 200-mesh nickel grid. Oxidation states of the catalyst metals were analyzed by a KRATOS Axis Ultra DLD X-ray photoelectron spectrometer with a monochromated Al K$\alpha$ X-ray source ($h\gamma$ = 1486.5 eV).


https://doi.org/10.1021/acsestengg.4c00203
ACS EST Engg. 2024, 4, 2186−2197

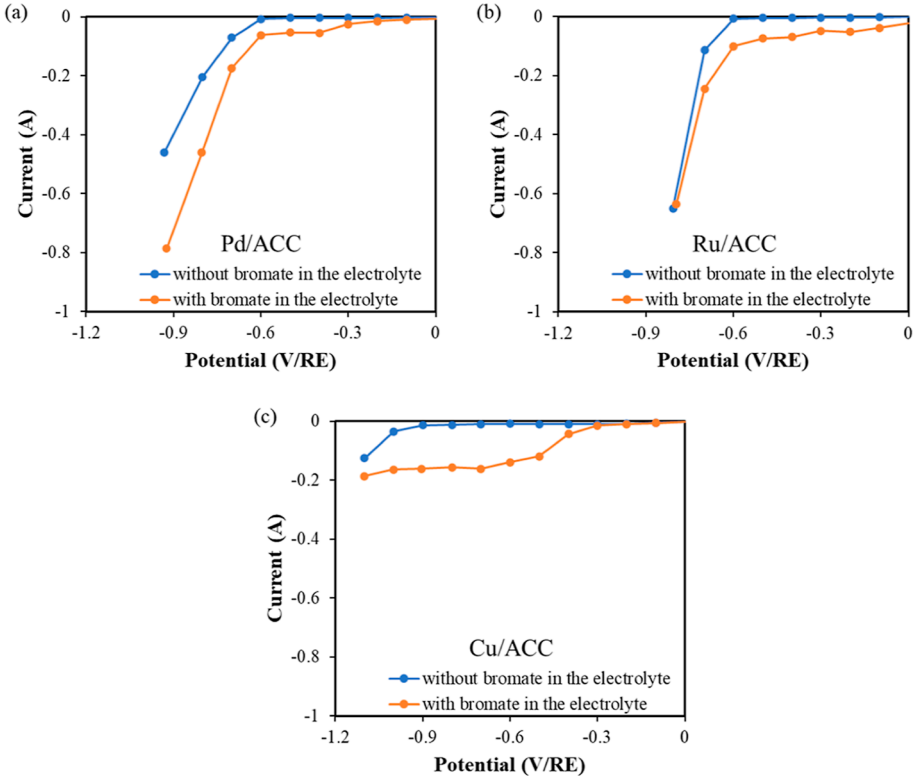


**Figure 2.** Current density−potential curves from multistep CA for (a) Pd/ACC, (b) Ru/ACC, and (c) Cu/ACC in the PPTL flow reactor using a 0.02 M PW alone and amended with 200 $\mu$g/L bromate, recirculated at 40 mL min$^{-1}$. Optimal potentials that minimize HER and maximize BRR are apparent for Pd/ACC, Ru/ACC, and Cu/ACC at −0.6 V/RE, −0.6 V/RE, and −0.7 V/RE, respectively.

The recorded spectra were processed by CasaXPS software to deconvolute the peaks and determine the catalyst compositions. Samples for XPS were prepared using the same procedures as the cathode preparation by drop-casting catalysts on ACC, dried in the oven, and then reduced by $N_2$ and $H_2$ flows in a furnace channel.

**2.5. Cost Estimation of Bromate Treatment in Drinking Water.** The cost for bromate treatment using IX, GAC, RO, and EC was estimated for a drinking water treatment plant processing 0.5 million gallons per day (MGD). This was done by assuming the initial bromate concentration to be 0.2 mg/L and treated to be ∼0.01 mg/L. This also assumed that bromate treatment occurred after all other treatment processes. Estimated costs are normalized to 1000 gallons of treated water. Costs for IX, GAC, and RO were estimated using the work breakdown structure-based cost model (WBS model) from the U.S. Environmental Protection Agency.[35−37] Costs for EC were estimated based on material used (anode and membrane) and the catalyst metal and energy consumption values obtained from this study. Costs for cathode regeneration were not included because further work is needed to determine regeneration details during long-term bromate treatment. Catalyst metal costs were calculated from experimentally determined bromate reduction rates, targeted initial and final bromate concentrations, and the water treatment plant flow rate. The WBS model includes direct capital costs (total costs of individual items of capital equipment), add-on costs (permits, pilot study, and land acquisition costs), indirect capital costs, and annual operating and maintenance (O&M) costs. Add-on costs, indirect capital costs, and general direct costs (e.g., piping and pumping system costs for influent and effluent) were excluded so that cost comparisons to EC were as fair as possible.

## 3. RESULTS AND DISCUSSION

**3.1. Pd, Ru, and Cu on ACC Are Primarily Metallic.** Loadings of Pd, Ru, and Cu on the three cathodes (i.e., Pd/ACC, Ru/ACC, and Cu/ACC) determined from ICP-OES are presented in Table S3 and are 0.90 ± 0.00, 1.69 ± 0.80, and 1.34 ± 0.34 wt %, respectively. The target deposition amount for each catalyst was 1 wt %. PXRD spectra for ACC, Pd/ACC, Ru/ACC, and Cu/ACC are shown in Figure 1a. The characteristic peaks at 30.7 and 43.7° for C(002) and C(100), respectively, are from crystalline carbon in ACC, and they are observed in all three cathodes. The Pd peaks (111), (200), (220), (311), and (222), Ru peaks (100), (002), (101), (102), and (110), and Cu peaks (111), (200), and (220) are observed on Pd/ACC, Ru/ACC, and Cu/ACC, respectively.[15,38,39] Low resolution TEM images of Pd/ACC, Ru/ACC, and Cu/ACC are shown in Figures 1b and S2a,b, respectively. For each cathode, a small piece of ACC with at least 30 catalyst nanoparticles was evaluated, and the obtained particle distributions are also presented in Figures 1b and S2a,b. The median sizes of Pd, Ru, and Cu nanoparticles are 13.7, 5.1, and 9.8 nm, respectively. Pd nanoparticles formed larger aggregates in some locations, resulting in their larger median size, and Ru nanoparticles were the most dispersed, with the smallest sizes.

XPS spectra aided in the determination of the oxidation state of the catalysts after thermal treatment. The deconvolution of Pd $3d_{5/2}$ peak at 336.6 eV results in two peaks at 336.5 and 337.5 eV (Figure S2a), indicating the presence of PdO and $PdO_2$, respectively.[40] Ru $3d_{5/2}$ peak at 285.2 eV was


https://doi.org/10.1021/acsestengg.4c00203
ACS EST Engg. 2024, 4, 2186−2197

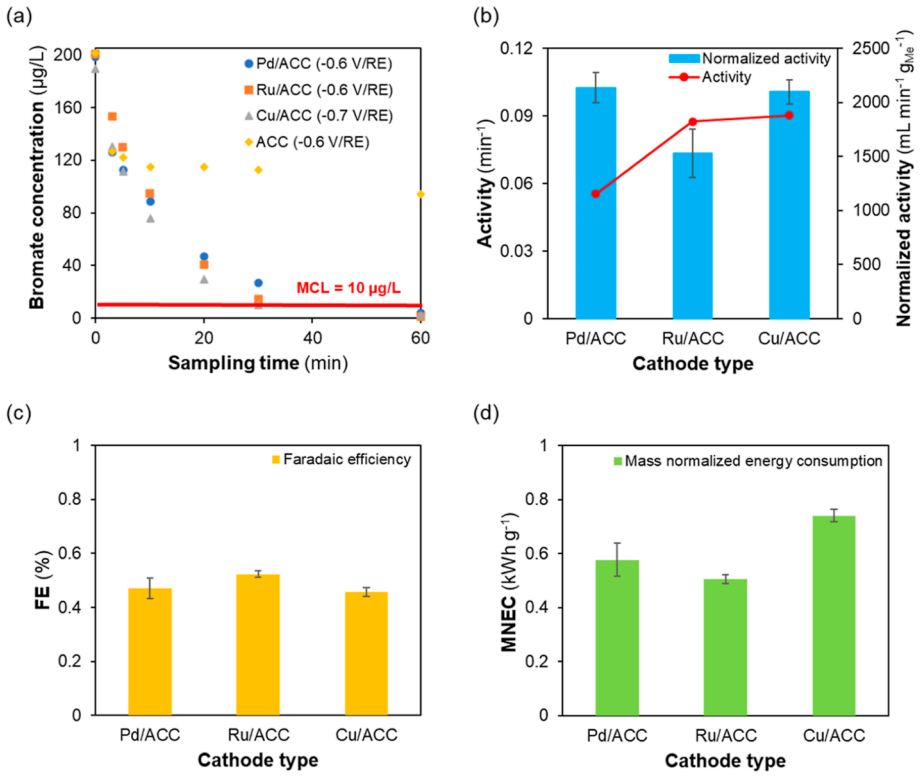


**Figure 3.** (a) Bromate concentrations over time with Pd/ACC at −0.6 V/RE, Ru/ACC at −0.6 V/RE, and Cu/ACC at −0.7 V/RE in 0.02 M PW and addition of 200 $\mu$g/L bromate at 40 mL min$^{-1}$ in the PPTL flow reactor. (b) Activity and normalized activity, (c) FE, and (d) mass normalized energy consumption (MNEC) values for bromate reduction with Pd/ACC, Ru/ACC, and Cu/ACC in 0.02 M PW and addition of 200 $\mu$g/L bromate at 40 mL min$^{-1}$ in the PPTL flow reactor.

deconvoluted to show two peaks at 281.1 and 282.0 eV (Figure S2b) as evidence of Ru and $RuO_2$ formation, respectively, and a small peak at 282.9 eV for RuOx.[41] Two peaks found in the XPS spectrum for copper catalysts were at 932.9 and 952.8 eV. Deconvolution of Cu $2p_{3/2}$ peak leads to $Cu/Cu^+$ and $Cu^{2+}$ peaks at 932.9 and 934.2 eV (Figure S2c), respectively.[42] Furthermore, a peak found in the Cu LMM Auger spectrum identified the presence of $Cu^0$ and $Cu^+$ peaks at 916.3 and 917.9 eV, respectively (Figure S2d);[42] hence, Cu, $Cu_2O$, and CuO are the main forms in the prepared catalysts.

Overall, the results indicate that all three metals are present as nanoparticles on the ACC electrode. Metals and their oxides are evident in the PXRD and XPS spectrum, indicating the incipient wetness impregnation method reduces catalyst metals to both their zerovalent and oxidized state. We note that metal oxides are likely formed upon Me exposure to air during sample preparation and that these oxides are likely reduced to Me when subject to a strong reducing current just prior to bromate reduction in the PPTL flow reactor.

**3.2. Optimal Potentials for Bromate Reduction with Minimal Hydrogen Evolution Are Determined.** Multistep CA experimental results for Pd/ACC, Ru/ACC, and Cu/ACC are presented in Figure 2. For Pd/ACC (Figure 2a) without added $BrO_3^-$, the current density is close to zero from 0.0 to −0.6 V/RE and markedly increases (i.e., becomes more negative) below −0.6 V/RE, indicating the onset of HER. With added bromate, the current density gradually increases between 0.0 and −0.6 V/RE and then markedly increases below −0.6 V/RE with HER. The gradual increase of current density between 0.0 and −0.6 V/RE indicates bromate reduction occurring within this applied potential range without HER. For Ru/ACC (Figure 2b), very similar results were obtained compared to those for Pd/ACC, except that current density started to increase with added bromate at a higher applied potential range (0.0 ∼ −0.4 V/RE), which resulted from BRR, and the current density without and with added bromate converges at the lowest applied potential (−0.8 V/RE), indicating that HER is dominating over BRR at this potential. For Cu/ACC (Figure 2c) without added bromate, the current density does not start to slightly increase as a result of HER until below −0.7 V/RE and then only markedly increases below −0.9 V/RE. The results indicate that more current is generated with added bromate at potentials above those that promote HER compared to both Pd/ACC and Ru/ACC.

PGMs are known as excellent hydrogenation catalysts and promotors of HER,[43] and this is supported by the multistep CA results that show HER onset at less negative applied potentials for Pd/ACC and Ru/ACC (i.e., −0.6 V/RE) compared to Cu/ACC. Conversely, Cu is known as a relatively poor hydrogenation catalyst,[44] and HER is only observed at more negatively applied potentials (<−0.9 V/RE). The superior performance of Cu/ACC in promoting bromate reduction at potentials above the onset of HER is consistent with earlier studies,[19] showing this catalyst can direct more current toward BRR compared to HER at appropriate applied potentials. It should be noted that the current does not show much variation from −0.7 to −0.9 V/RE on Cu/ACC because the reaction rate remains constant in this potential range. Since BRR was the dominant reaction in the experiment, it is inferred that a bromate transfer flux from the bulk solution to the surface of the electrode in the reactor was not increased as the


https://doi.org/10.1021/acsestengg.4c00203
ACS EST Engg. 2024, 4, 2186−2197

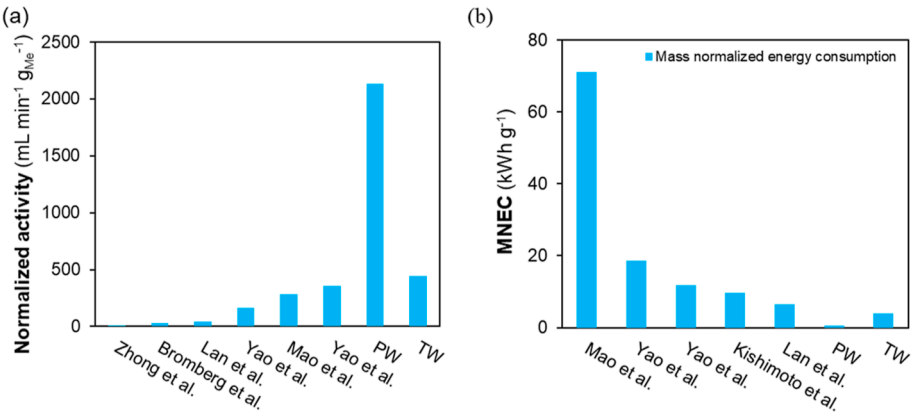


**Figure 4.** Comparison of (a) normalized activity and (b) MNEC values for bromate reduction with previous studies and this work done in PW and TW on electrocatalytic bromate reduction.

potential increased. This suggests that there is a bromate mass-transfer limitation in the reaction environment. Overall, the results indicate that to maximize BRR and minimize HER the optimal applied potentials are −0.6, −0.6, and −0.7 V/RE for Pd/ACC, Ru/ACC, and Cu/ACC, respectively.

**3.3. Electrocatalytic Bromate Reduction Kinetics Are Faster Than Any Reported Values.** Electrocatalytic bromate reduction kinetics were measured at the aforementioned optimal potentials (Section 3.2) in the PPTL flow reactor. Concentrations of bromate versus time are shown in Figure 3a. The initial bromate concentration of 200 $\mu$g/L was electrocatalytically reduced to below the MCL (i.e., 10 $\mu$g/L) in 1 h with each of the three electrodes, i.e., Pd/ACC, Ru/ACC, and Cu/ACC, indicating all three have similarly high bromate reduction activities. Bromate removal tests with and without catalysts loaded onto ACC were performed for comparison (Figure S3). Although 53% of bromate removal was observed without Pd loading, only 26% of bromate was reduced to bromide and 27% of Br species were adsorbed to the cathode in a 1 h experiment. A drop in mass balance of Br species was observed during electrocatalytic bromate reduction with Pd/ACC at −0.6 V/RE in the first 20 min, likely due to bromate adsorption and/or the formation/adsorption of intermediates, as shown in Figure S3b. Bromate reduction intermediates $BrO_2$, $HBrO_2$, and HBrO were reported in Qu's work during electrocatalytic bromate reduction;[45] these would be reduced to $Br_2$, and immediately reduced to $Br^-$ at −0.6 V/RE ($E^0$ for $Br_2$ = 1.09 V/NHE[46]). Hence all of the reduced bromate formed the final product, $Br^-$.

Pseudo-first-order rate constants without and with normalization to the metal loading were determined from concentration decay profiles and are shown in Figure 3b, and listed in Table S4. They are 0.0554 ± 0.0036, 0.0875 ± 0.0098, and 0.0903 ± 0.0094 $min^{-1}$ for Pd/ACC, Ru/ACC, and Cu/ACC, respectively, without normalization, and 2136 ± 139, 1530 ± 222, and 2097 ± 136 mL $min^{-1}$ $g_{Me}{}^{-1}$, respectively, with normalization. Without normalization to metal loading, Pd/ACC has the lowest activity, and Ru/ACC and Cu/ACC have similar activity. However, with normalization, this trend shifts. Ru/ACC has the lowest normalized activity, and the normalized activities for Pd/ACC and Cu/ACC are similar. In prior work, Pd is the most common electrocatalyst,[17,20,47] and direct comparisons of bromate reduction activity among all three metals are not available. In one study, however, Ru and Cu on a carbon nanotube support in a double-chamber electrochemical PTFE reactor were directly compared, and extents of bromate reduction were within 7% of each other after 2 h of reaction.[19] Although PGMs generally exhibit higher normalized activities for oxyanion reduction than other metals due to atomic hydrogen assisting indirect electron transfer, Cu/ACC has comparable activity for bromate reduction to Pd/ACC. Two possible reasons are that Cu nanoparticle sizes are smaller than Pd[48] and that a more negative potential was applied to Cu/ACC than Pd/ACC. Discerning the exact reasons requires further study.

Normalized bromate reduction activities in PW for Pd/ACC from this work are compared to literature values in Figure 4a and Table S5; values in this work are 6 to 71 times greater than literature values. A primary reason for this marked improvement in normalized activity is the practical elimination of the mass-transfer limitations in the PPTL flow reactor. We conducted electrochemical experiments in a PPTL flow reactor to study its limiting current and evaluate the mass-transfer rate. The mass-transfer coefficient was found to be $4.66 \times 10^{-5}$ m $s^{-1}$ and used to determine the second Damköhler number, which describes the ratio of reaction rate to mass-transfer rate. A small second Damköhler number (0.02) indicates that mass transfer was faster than the reaction for bromate reduction in the PPTL flow reactor. This is supported by modeling results in Yan's work, which determined that the dimensionless mass-transfer coefficient, Nu, is greater than the dimensionless reaction rate constant, $K_w$, for nitrite reaction in the PPTL flow reactor by a factor of 3.5, suggesting the overall reaction rate with Pd/ACC in the PPTL flow reactor is reaction and not mass-transfer limited.[15] To further investigate the influence of reactor design and mass-transfer resistance on the activity, we also evaluated the limiting current and mass-transfer coefficient in the H-cell and determined that the mass-transfer coefficient is 2.6 times greater in the PPTL flow reactor than in the H-cell. This indicates that the continuous flow mode PPTL flow reactor used in this study provided faster mass transfer and improved normalized activity compared to batch reactors, in which most previous works were done.[49] In support of this assertion, a thin-film reactor was found to have higher reaction rates than a batch reactor for glycerol conversion.[50]

We note that the high surface area of the supporting electrode and small Pd particle sizes can improve electrocatalytic activity; however, the electrode surface area and catalyst particle sizes are similar to those of other studies (see Table S5), and no clear trend in bromate reduction activity


https://doi.org/10.1021/acsestengg.4c00203
ACS EST Engg. 2024, 4, 2186−2197

normalized by these values is apparent. Alternatively, our approach to use phosphate buffer as an electrolyte could enhance bromate reduction activity compared to other studies. BRR is more active at lower pH, and phosphate buffer maintains a solution pH near neutral because of its close $pK_{a_2}$ (i.e., 7.2). By contrast, sodium sulfate was used to control the ionic strength in most other studies (Table S5); it provided practically no buffering capacity, allowing the pH to increase during reactions.

**3.4. FE of Bromate Reduction.** FE values for Pd/ACC, Ru/ACC, and Cu/ACC in PW are shown in Figure 3c and listed in Table S4. The FEs for all three catalysts when treating 200 $\mu$g/L bromate are very small, between 0.46 and 0.52%. The lowest FE is with Cu/ACC (0.46%), indicating only 0.46% of electrons were transferred to BRR while the rest contributed to other reactions, which may include hydrogen adsorption reactions, metal oxide reduction reactions, oxygen reduction reactions, and water electrolysis. We note that FEs are much lower than those reported for other pollutants like nitrate and nitrite. For example, the FE in the same reactor with nitrite was 51%.[15] However, the initial nitrite concentration was 100,000 $\mu$g/L, and the higher starting concentration likely explains the difference. To explore this effect, CA experiments were also performed using only Pd/ACC with bromate concentrations at 1000 and 12,790 $\mu$g/L, and results are listed in Table S6. As expected, FEs increase from 0.47 to 2.3 and to 21% with initial concentrations of 200, 1000, and 12,790 $\mu$g/L, respectively. This effect is well established and is due to the greater reactant concentration gradient and mass flux to the cathode surface at greater concentration, providing more reactant to accept electrons compared to competing reactions.[51]

**3.5. Energy Consumption of Bromate Reduction.** While poor FE is a concern, the primary indicator of electrocatalytic energy efficiency is the total energy consumed by reducing bromate from the initial concentration to 10 $\mu$g/L per gram of reduced bromate, referred to as MNEC; the results are shown in Figure 3d for treating 200 $\mu$g/L bromate and listed in Table S4 for all initial bromate concentrations. MNEC values for 200 $\mu$g/L initial bromate with Pd/ACC, Ru/ACC, and Cu/ACC cathodes are 0.576 ± 0.061, 0.505 ± 0.016, and 0.740 ± 0.029 kW h g$^{-1}$, respectively. Interestingly, Cu/ACC with the highest normalized activity does not have the lowest MNEC because the total applied potential for Cu/ACC was higher than those for Ru/ACC and Pd/ACC. MNEC results for treating different initial bromate concentrations with Pd/ACC are also listed in Table S6. Not surprisingly, the lowest MNEC for bromate reduction, 0.013 kW h g$^{-1}$, coincides with the greatest initial bromate concentration (i.e., 12,790 $\mu$g/L), and these values increase with decreasing initial bromate concentration.

MNEC values for electrocatalytic bromate treatment in this study are compared to those reported in the literature in Figure 4b, with actual values listed in Table S5. MNEC values range from 5.1 to 24.93 kW h g$^{-1}$, and values when using PW in this study are 9−43 times lower than the reported values in the literature. We attribute this difference to both avoiding high energy consumption for HER by potential control and the thin-film design of the PPTL flow reactor that minimizes ohmic resistance in the reaction chamber, thus significantly reducing energy consumption for BRR. Additionally, the higher normalized activity of bromate reduction in our work compared to other studies also contributes to low energy consumption demand. This result is important because energy consumption is one of the key metrics that determines the technology's feasibility.

**3.6. Long-Term Reactor Performance.** Long-term reactor performance was assessed by performing five bromate reduction experiments in series using the same PPTL flow reactor and Pd/ACC electrode with the cathodic feed solution containing fresh bromate at 200 $\mu$g/L replaced before each cycle. The Pd/ACC electrode was chosen for long-term performance assessment because in single-cycle tests, Cu/ACC showed much greater leaching (42.378 $\mu$g/L for Cu versus 0.354 $\mu$g/L for Pd) and because normalized bromate reduction rates for Pd/ACC are 40% greater than for Ru/ACC. As expected based on results in other studies,[15,52] the normalized reduction rate constant decreases with each cycle, decreasing the most between cycles 1 and 2 and then more gradually between cycles 2 and 5, as shown in Figure 5. Reasons for Pd

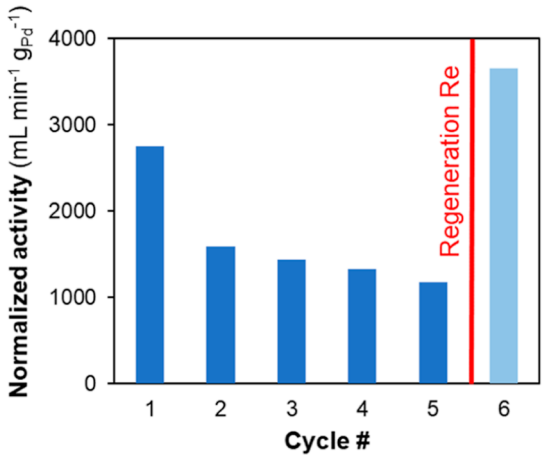


**Figure 5.** Normalized activities for 6 cycles of electrocatalytic bromate reduction at −0.6 V/RE in 0.02 M PW with 200 $\mu$g/L initial bromate at 40 mL min$^{-1}$ in the PPTL flow reactor.

catalyst deactivation have been speculated in prior work and include catalyst leaching, surface blocking with adsorbed species (e.g., NOM), surface poisoning with covalently bound reduced sulfur species, nanoparticle aggregation, and surface oxidation to form Pd oxides.[53,54] Very little Pd leached after the first cycle (<0.00134% of initial Pd), indicating this is not the main reason. Surface blocking and poisoning are unlikely because PW was used. In a prior study with multiple treatment cycles and catalyst deactivation, Pd nanoparticle aggregation was not observed using TEM, and PdO species formation was not evident from XPS spectra;[52] the latter could have been due to poor sensitivity from dilute Pd atoms on the catalyst support. In a related study using Cu/ACC for nitrate reduction, XPS was used to show that more CuO species were present after five sequential reduction cycles that showed deactivation.[55] Hence, the formation of more Pd oxide species with deactivation is a possibility.

Pd/ACC regeneration was performed after the fifth bromate reduction cycle by applying a more negative reduction potential (∼−1.2 V/RE) for 1 h, followed by a single-cycle bromate reduction experiment. Surprisingly, the recovered normalized bromate reduction activity is greater than the original normalized bromate reduction activity in the first cycle. This suggests that some surface oxidation was present


https://doi.org/10.1021/acsestengg.4c00203
ACS EST Engg. 2024, 4, 2186−2197

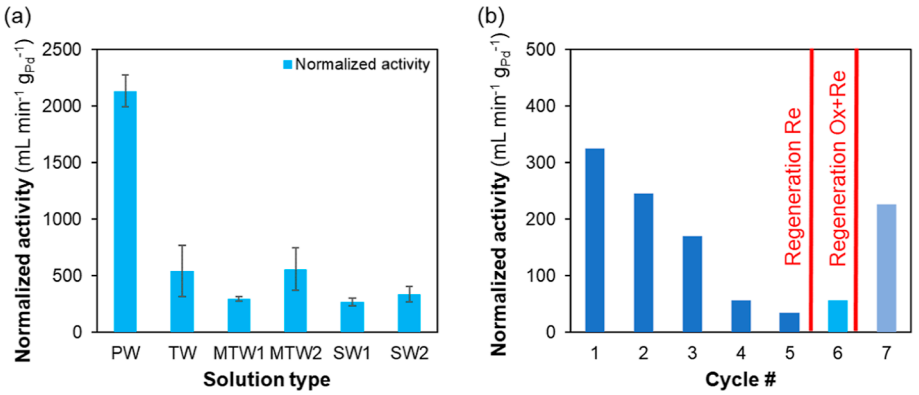


**Figure 6.** Normalized activities for (a) electrocatalytic bromate reduction in various solution types, PW, TW, MTW1, MTW2, SW1, and SW2 and (b) 5 cycles of electrocatalytic bromate reduction in TW at −0.6 V/RE with 200 $\mu$g/L initial bromate at 40 mL min$^{-1}$ in the PPTL flow reactor followed by 1 cycle after reductive regeneration for 1 h (Re, −1.2 V/RE) and 1 cycle after oxidative (Ox, +0.6 V/RE) and reductive regeneration (Re, −1.2 V/RE) for 0.5 h each.

before the first reduction cycle, and this increased during treatment cycles; this was reversed when a more negative potential was applied for regeneration. To investigate the reason for greater activity on regenerated versus freshly prepared Pd/ACC, TEM images for fresh and regenerated samples were compared and used to examine changes in the particle size and morphology. Results are presented in Figure 1b,c, along with Pd size distributions. No significant changes in particle size or morphology are apparent compared with freshly made Pd/ACC (Figure 1b). Round and rod-shaped Pd nanoparticles were observed in both samples. Anecdotally, individual Pd particles appear more congregated and in larger groupings in fresh Pd/ACC, versus more dispersed in regenerated Pd/ACC. It is possible this gave rise to more accessible Pd surface area in regenerated Pd/ACC, but it was not possible to meaningfully quantify this effect with the number of TEM images acquired. We note that other regeneration strategies might be needed for other fouling mechanisms. For example, both a strongly oxidative and a strongly reductive cycle might be needed to reverse catalyst poisoning with reduced sulfur species,[25] and treatment with a base might be required to remove NOM.[8] Regardless, the results show that catalyst longevity can be maintained after deactivation in PW by applying only a strongly negative potential for regeneration.

**3.7. Electrocatalytic Treatment for Bromate Reduction in TW.** Actual, adjusted, and synthetic tap waters were used in place of PW to determine whether normalized bromate reduction activity, FE, and MNEC with Pd/ACC are promising in more complex water matrices that we might expect in drinking water treatment plants. TW was collected immediately before each reduction experiment to ensure that no chemical or biological reactions occurred with TW storage that could change water quality. Water was collected after the tap was flushed for several minutes to avoid stagnant pipe water. Two modified tap water (MTW) were used. The first, MTW1, is TW with $K_2SO_4$ added to increase the ionic strength by 0.002 M; this was done to evaluate the effects of solution resistance on energy consumption. The second, MTW2, is TW treated with 0.5 M $H_2SO_4$ so the pH matched that for PW since pH affects surface charge and possibly bromate adsorption to reactive sites. Two additional synthetic tap waters (SW) with the same ionic strength and pH as the TW were prepared. The first, SW1, was prepared with phosphate salt ($K_2HPO_4$), and the second, SW2, was prepared with carbonate salt ($NaHCO_3$), followed by pH adjustment with KOH and NaOH since the carbonate buffer in TW can impact reduction differently than a phosphate buffer. The concentrations of phosphate and carbonate in SW1 and SW2 were 0.0023 and 0.0052 M, respectively, and were calculated to match the ionic strength of TW at a pH equal to 9.5.

Normalized bromate reduction activity is shown in Figure 6a, and FE and MNEC results for the different water sources are presented in Table S4. The normalized bromate reduction activities with TW, MTW1, MTW2, SW1, and SW2 are 544 ± 229, 295 ± 20, 560 ± 186, 267 ± 35, and 337 ± 66 mL min$^{-1}$ $g_{Pd}^{-1}$, respectively. These are 25, 14, 26, 13, and 16% of that for PW. Interestingly, FE and MNEC values for these water sources qualitatively scale with normalized bromate reduction activities, such that FEs for TW, MTW1, MTW2, SW1, and SW2 are 38, 26, 60, 22, and 30% of that for PW, respectively, and MNEC values are 381, 437, 203, 522, and 389% of that for PW, respectively.

Comparing TW to PW, TW had a lower normalized bromate reduction activity than PW. Previous studies have shown that pH, ionic conductivity, electrolytes, buffer capacity, and catalyst poisoning compounds have a significant impact on the electrocatalytic activity.[56−58] The normalized activity for MTW1 (added IS) was lower than that for TW. It is possible that the complexity of the TW matrix had side reactions with the addition of electrolytes, forming complexes and precipitants that interrupted and hindered BRR (e.g., $CaSO_4$, $Ca(OH)_2$). The normalized activity for MTW2 (lower pH) was only slightly greater than TW. Although the addition of chemicals in TW affected BRR negatively, the benefit from a lower pH solution are expected to enhance activity since BRR is a pH-dependent reaction and is promoted by lower pH.[59] It should be noted that solution buffer capacity was lowered when the pH of TW was adjusted because the original TW pH of 9.5 is near the carbonate system $pK_{a_2}$ (10.33); this also could have affected bromate reduction activity. To explore this effect, results from SW1 (phosphate buffer) and SW2 (carbonate buffer) at the pH of TW were compared. At pH 9.5, SW1 has little buffer capacity since the closest $pK_{a_3}$ for the phosphate system is 12.32, while SW2 is well buffered near the carbonate system $pK_{a_2}$; as expected, the normalized activity with SW1 is lower than that with SW2. Overall, the results suggest that both


https://doi.org/10.1021/acsestengg.4c00203
ACS EST Engg. 2024, 4, 2186−2197

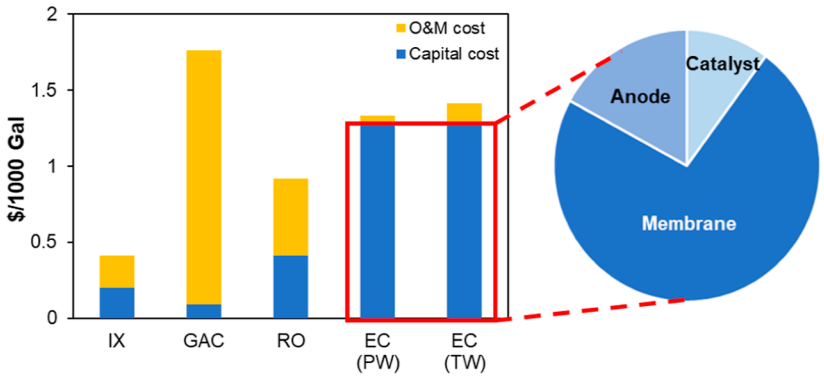


**Figure 7.** Costs assessment of bromate reduction per 1000 gallons of treated water with IX, GAC, RO, and EC treatment. The bar chart shows the capital and O&M costs for each treatment type and the pie chart shows the capital costs for each material. EC capital costs are amortized over 20 years, while IX, GAC, and EO capital costs are amortized over 26.1, 20.1, and 23.6 years, respectively, as indicated in the WBS model. Electricity cost is $0.105/kW h for all treatment types. All costs are converted to Producer Price Index 2023.

buffer capacity and pH play important roles in the kinetics of BRR. Given that the buffer in TW is a carbonate system, one applicable strategy from the results to enhance the activity for BRR is to lower the pH below 6.33, the $pK_{a_1}$ value for the carbonate system, so that buffer capacity can be increased and the pH is decreased.

The normalized bromate reduction activity and MNEC values for bromate in TW with Pd/ACC are compared with the literature values in Figure 4. Despite poorer bromate reduction performance in TW compared to PW, the normalized bromate reduction activity and MNEC values for bromate in TW are better than those for all literature studies to date, where literature studies were mostly performed in synthetic waters. This highlights the superior performance of PPTL flow reactor compared to other reactor designs in the literature and the importance of overcoming mass-transfer limitations.

Long-term reduction performance was also studied in TW to investigate the viability of cathode regeneration with a negative applied potential; normalized activities for six cycles are shown in Figure 6b. Similar to long-term reduction performance in PW, activity dropped after the first cycle and gradually decreased with additional cycles. The negative potential regeneration process after the fifth cycle exhibited only a slight increase of normalized activity on the cathode for bromate reduction, which could potentially be caused by possible poisoning compounds (CO, $S^{2-}$, etc.) for Pd in TW. McPherson's work indicated that cyclic voltammetry was able to oxidize contaminants that occupied Pd active sites and release the catalysts poisoning compounds.[60] By applying an oxidative potential first, followed by a reductive potential on the cathode after cycle 6, much of the original normalized activity for BRR was recovered (in cycle 7), indicating a promising strategy for in situ regeneration of the electrode in drinking water treatment. Although activity can be regenerated, a more frequent regeneration of the cathode and longer term, continuous flow tests are necessary for treating TW since poisoning compounds could deactivate the catalyst drastically. On the other hand, several studies focused on the modification of catalysts to enhance stability over long-term operation, and this could be a promising strategy to treat real water matrices.[61−63]

An interesting observation is that the range of normalized bromate reduction activities for TW is 234 to 800 mL $min^{-1}$ $g_{Pd}^{-1}$, much greater than the relative range for any synthetic TW. We note that TW collected on different days for replicate tests had consistent conductivity and pH, but it is possible that concentrations of minor species varied and affected normalized bromate reduction activity (e.g., residual chlorine, nitrite). This remains an important topic for future study.

**3.8. Cost Assessment of Bromate Reduction in Various Technologies.** Capital and O&M costs of bromate treatment with IX, GAC, and RO, as well as material (membrane and anode), Pd metal, and energy costs of bromate treatment with EC, all per 1000 gallons of treated drinking water, are presented in Figure 7 for a 0.5 MGD drinking water plant. Capital and O&M costs for IX, GAC, and RO were determined using the WBS model, and input parameters are provided in Texts S1−S3. Key assumptions for IX are strong base polystyrenic macroporous resins with empty bed contact time (EBCT) of 12 min, and the constants for the Freundlich isotherm model are from Xu's work.[64] Langmuir adsorption model fitting parameters for bromate on activated carbon in Yan's work and an EBCT of 8 min were used as key assumptions for GAC.[65] A low pressure RO membrane with a rejection rate of 85% is the main assumption for RO. Equations for calculating catalyst and energy costs for EC are described in Text S4. Key assumptions are that bromate reduction activities in PW and TW are used for determining treatment time to reduce bromate from 200 to 10 $\mu$g/L and that 11.7% of Pd is lost per year and requires replacement. The latter assumption is determined by estimation based on the aforementioned Pd leaching test (Section 3.6) and accounted for the expense of capital cost to maintain the same Pd loadings annually. This assumption requires further validation via long-term reactor operation tests. Note that material, Pd metal, and energy costs are surrogates for capital and O&M costs, respectively, because these are expected to dominate these categories[66] and because other capital and O&M costs are not available for this emerging technology.

Capital costs for IX, GAC, and RO, EC are $0.20, 0.09, 0.41, and 1.29/1000 gallon of treated water, respectively. RO requires antiscalant pretreatment, and the membrane itself has a much higher capital cost than IX and GAC. GAC has the lowest capital cost due to the ease of manufacturing these adsorbents. EC has the highest capital cost. Among the materials in capital cost, catalysts contribute the least ($0.13/1000 gallon of treated water) and Nafion membrane the most ($0.94/1000 gallon of treated water). The Nafion membrane


https://doi.org/10.1021/acsestengg.4c00203
ACS EST Engg. 2024, 4, 2186−2197

cost can be reduced to below half of the market price based on the TNO's electrochemical model and was calculated by assuming that the membrane price is proportional to its thickness.[67] We note that EC costs have a higher uncertainty; they may be overestimated because they are based on a small-scale reactor with retail material prices or they may be underestimated because only main capital costs are considered.

The O&M costs for IX, GAC, and RO, EC are $0.21, 1.67, 0.51, and 0.04/1000 gallon of treated water, respectively. GAC, surprisingly, has the highest O&M cost due to the relatively low capacity of GAC to adsorb bromate, which leads to a recurrent need for GAC replacement and disposal of the waste. IX O&M costs are lower because this material has a higher adsorption capacity for bromate and requires less frequent resin regeneration. RO O&M costs are higher due to chemical treatments needed to address membrane fouling and the energy used for high-pressure pumps. For EC treatment, the only O&M cost considered is the power supplied for reactor operation. Pd replacement costs could have been put in this category but are considered in capital costs. The low O&M cost indicates that energy demands for achieving high bromate removal in the EC reactor are practically negligible. This is highlighted by comparing the energy cost for EC in PW and TW (Figure 7); the O&M costs for the latter are three times the former but still only a small fraction of the total costs. Also, unlike IX, GAC, and RO, regeneration or disposal of a waste stream is not necessary. Further, the cathode can be regenerated in situ, so treatment can continue almost uninterrupted at a water treatment plant. While these results show the technical advantages and low to comparable costs of EC treatment, a pilot study is needed to determine how technical performance and cost scale and to evaluate EC performance over many continuous weeks to months of operation.

## 4. CONCLUSIONS

Results from this study reveal improvements in normalized activity (6−71 times higher than other studies) and total energy consumption per gram of bromate removed (9−43 times lower than other studies) for electrocatalytic reduction of bromate compared to literature values. A Pd-based cathode has the highest normalized activity (2136 mL $min^{-1}$ $g_{Pd}^{-1}$) compared to Cu- and Ru-based cathodes, with very little leaching (ca. 0.000014 mg of Pd leaching in 1 h during the treatment process) and low MNEC (0.576 kW h $g^{-1}$) in a custom-designed PPTL flow reactor. Although normalized bromate reduction activity decreases with repeated treatment cycles, the Pd-based cathode is also robust to in situ regeneration, which regains much of the original normalized activity. The capital and O&M costs for treating 1000 gallons of TW using the Pd-based PPTL flow reactor are $1.29 and $0.12, respectively. The O&M cost, which represents electricity input, is only a small fraction of the total, resulting in only a small change in the total costs when treating an ideal solution or Austin TW.

Comparing costs with other technologies for bromate treatment, EC has the highest capital but lowest O&M costs, with total costs that are lower than GAC and higher than RO and IX. High costs for GAC are due to poor bromate adsorption leading to frequent GAC replacement and waste disposal. High costs for RO are due to pumping energy demands and chemical treatment to address fouling. High costs for EC are due to the Nafion membrane and the $IrO_2$-based anode, and future research could address replacing these expensive materials. IX, GAC, and RO all produce waste streams; we currently assume that these waste streams can be disposed of at some average price, but these costs vary widely by region and can drive costs upward. Also, if treatment of these waste streams is required, costs for these technologies can increase further. In contrast, EC treatment produces no waste stream and can reduce bromate from any relevant concentration to below the MCL. In summary, EC treatment for bromate appears very promising and is ready for pilot scale assessment of scale up and long-term reactor operation.

## ■ ASSOCIATED CONTENT

### Supporting Information

The Supporting Information is available free of charge at https://pubs.acs.org/doi/10.1021/acsestengg.4c00203.

Additional materials and methods; schematic diagram and layout of PPTL flow reactor; data analysis; TEM images and XPS spectrum for Pd/ACC, Ru/ACC, and Cu/ACC; mass balance of bromate and bromide over time; published chemical and physical properties of ACC; constituents of Austin TW in the third quarter; catalyst loadings on ACC; normalized activity, FE, and MNEC values of electrocatalytic bromate treatment in different solutions; comparison of the physical properties of electrode, experimental parameters, normalized activity, FE, and MNEC values for electrocatalytic bromate reduction in different studies; normalized activity, FE, and MNEC values of electrocatalytic bromate treatment with different initial bromate concentrations by Pd/ACC; and cost estimation of bromate treatment in drinking water with GAC, IX, RO, and EC (PDF)

## ■ AUTHOR INFORMATION


### Corresponding Author

**Charles J. Werth** − *Maseeh Department of Civil, Architectural and Environmental Engineering, The University of Texas at Austin, Austin 78712 Texas, United States;* orcid.org/0000-0002-8492-5523; Email: werth@utexas.edu

### Authors

**Kuan-Lin Lee** − *Maseeh Department of Civil, Architectural and Environmental Engineering, The University of Texas at Austin, Austin 78712 Texas, United States;* orcid.org/0009-0005-9609-6426

**Chenxu Yan** − *Maseeh Department of Civil, Architectural and Environmental Engineering, The University of Texas at Austin, Austin 78712 Texas, United States; Carollo Engineers, Inc., Austin 78759 Texas, United States;* orcid.org/0000-0002-2227-5510

**Jingwen Xu** − *Maseeh Department of Civil, Architectural and Environmental Engineering, The University of Texas at Austin, Austin 78712 Texas, United States*

**Carolyn E. Brady** − *Department of Chemistry, The University of Austin at Texas, Austin 78712 Texas, United States*

Complete contact information is available at: https://pubs.acs.org/10.1021/acsestengg.4c00203


### Notes

The authors declare no competing financial interest.



https://doi.org/10.1021/acsestengg.4c00203
ACS EST Engg. 2024, 4, 2186−2197

## ■ ACKNOWLEDGMENTS

This work was supported by NanoCatRed (NORTE-01−0247-FEDER-045925) (ERDF—COMPETE 2020, —NORTE 2020, and—FCT under UT Austin Portugal), as well as from National Science Foundation under the award number CBET-1922504. The authors also thank Michelle Mikesh (UT Austin; LR-TEM), Dr. Hugo Celio (UT Austin; XPS), and Dr. Vincent Lynch (UT Austin; PXRD) for assistance with metal nanoparticle characterization.

## ■ REFERENCES

(1) Butler, R.; Godley, A.; Lytton, L.; Cartmell, E. Bromate environmental contamination: review of impact and possible treatment. *Crit. Rev. Environ. Sci. Technol.* **2005**, *35* (3), 193−217.
(2) Flanagan, E. *Ozone in Water Purification and Bromate Formation*; Water Online, 2021.
(3) Morrison, C. M.; Hogard, S.; Pearce, R.; Mohan, A.; Pisarenko, A. N.; Dickenson, E. R.; von Gunten, U.; Wert, E. C. Critical Review on Bromate Formation during Ozonation and Control Options for Its Minimization. *Environ. Sci. Technol.* **2023**, *57*, 18393−18409.
(4) Soltermann, F.; Abegglen, C.; Gotz, C.; Von Gunten, U. Bromide sources and loads in Swiss surface waters and their relevance for bromate formation during wastewater ozonation. *Environ. Sci. Technol.* **2016**, *50* (18), 9825−9834.
(5) Kirisits, M. J.; Snoeyink, V. L.; Kruithof, J. C. The reduction of bromate by granular activated carbon. *Water Res.* **2000**, *34* (17), 4250−4260.
(6) Gyparakis, S.; Diamadopoulos, E. Formation and reverse osmosis removal of bromate ions during ozonation of groundwater in coastal areas. *Sep. Sci. Technol.* **2007**, *42* (7), 1465−1476.
(7) Wiśniewski, J. A.; Kabsch-Korbutowicz, M. Bromate removal in the ion-exchange process. *Desalination* **2010**, *261* (1−2), 197−201.
(8) Liu, J.; Choe, J. K.; Sasnow, Z.; Werth, C. J.; Strathmann, T. J. Application of a Re-Pd bimetallic catalyst for treatment of perchlorate in waste ion-exchange regenerant brine. *Water Res.* **2013**, *47* (1), 91−101.
(9) Santos, A. S. G.; Restivo, J.; Orge, C. A.; Pereira, M. F. R.; Soares, O. S. G. Synthesis of monometallic macrostructured catalysts for bromate reduction in a continuous catalytic system. *Environ. Technol.* **2022**, *44*, 3834−3849.
(10) Cerrillo, J. L.; Palomares, A. E. A review on the catalytic hydrogenation of bromate in water phase. *Catalysts* **2021**, *11* (3), 365.
(11) Werth, C. J.; Yan, C.; Troutman, J. P. Factors impeding replacement of ion exchange with (electro) catalytic treatment for nitrate removal from drinking water. *ACS ES&T Eng.* **2021**, *1* (1), 6−20.
(12) Sanchis, I.; Diaz, E.; Pizarro, A.; Rodriguez, J.; Mohedano, A. Nitrate reduction with bimetallic catalysts. A stability-addressed overview. *Sep. Purif. Technol.* **2022**, *290*, 120750.
(13) Zheng, W.; Lee, L. Y. S.; Wong, K.-Y. Improving the performance stability of direct seawater electrolysis: from catalyst design to electrode engineering. *Nanoscale* **2021**, *13* (36), 15177−15187.
(14) Zhang, H.-X.; Wang, S.-H.; Jiang, K.; André, T.; Cai, W.-B. In situ spectroscopic investigation of CO accumulation and poisoning on Pd black surfaces in concentrated HCOOH. *J. Power Sources* **2012**, *199*, 165−169.
(15) Yan, C.; Kakuturu, S.; Butzlaff, A. H.; Cwiertny, D. M.; Mubeen, S.; Werth, C. J. Scalable reactor design for electrocatalytic nitrite reduction with minimal mass transfer limitations. *ACS ES&T Eng.* **2021**, *1* (2), 204−215.
(16) Yao, F.; Yang, Q.; Sun, J.; Chen, F.; Zhong, Y.; Yin, H.; He, L.; Tao, Z.; Pi, Z.; Wang, D.; et al. Electrochemical reduction of bromate using noble metal-free nanoscale zero-valent iron immobilized activated carbon fiber electrode. *Chem. Eng. J.* **2020**, *389*, 123588.
(17) Lan, H.; Mao, R.; Tong, Y.; Liu, Y.; Liu, H.; An, X.; Liu, R. Enhanced electroreductive removal of bromate by a supported Pd-In Bimetallic catalyst: kinetics and mechanism investigation. *Environ. Sci. Technol.* **2016**, *50* (21), 11872−11878.
(18) Yao, F.; Yang, Q.; Yan, M.; Li, X.; Chen, F.; Zhong, Y.; Yin, H.; Chen, S.; Fu, J.; Wang, D.; et al. Synergistic adsorption and electrocatalytic reduction of bromate by Pd/N-doped loofah sponge-derived biochar electrode. *J. Hazard. Mater.* **2020**, *386*, 121651.
(19) Wu, T.; Hu, J.; Wan, Y.; Qu, X.; Zheng, S. Synergistic effects boost electrocatalytic reduction of bromate on supported bimetallic Ru-Cu catalyst. *J. Hazard. Mater.* **2022**, *438*, 129551.
(20) Mao, R.; Zhao, X.; Qu, J. Electrochemical reduction of bromate by a Pd modified carbon fiber electrode: kinetics and mechanism. *Electrochim. Acta* **2014**, *132*, 151−157.
(21) Chen, P.-Y.; Yang, H.-H.; Huang, C.-C.; Chen, Y.-H.; Shih, Y. Involvement of Cu (II) in the electrocatalytic reduction of bromate on a disposable nano-copper oxide modified screen-printed carbon electrode: hair waving products as an example. *Electrochim. Acta* **2015**, *161*, 100−107.
(22) Song, Q.; Zhang, S.; Hou, X.; Li, J.; Yang, L.; Liu, X.; Li, M. Efficient electrocatalytic nitrate reduction via boosting oxygen vacancies of TiO2 nanotube array by highly dispersed trace Cu doping. *J. Hazard. Mater.* **2022**, *438*, 129455.
(23) Gravil, P.; Toulhoat, H. Hydrogen, sulphur and chlorine coadsorption on Pd (111): a theoretical study of poisoning and promotion. *Surf. Sci.* **1999**, *430* (1−3), 176−191.
(24) Wilke, S.; Scheffler, M. Poisoning of Pd (100) for the dissociation of H2: a theoretical study of co-adsorption of hydrogen and sulphur. *Surf. Sci.* **1995**, *329* (1−2), L605−L610.
(25) Chaplin, B. P.; Roundy, E.; Guy, K. A.; Shapley, J. R.; Werth, C. J. Effects of natural water ions and humic acid on catalytic nitrate reduction kinetics using an alumina supported Pd- Cu catalyst. *Environ. Sci. Technol.* **2006**, *40* (9), 3075−3081.
(26) Kopinke, F.-D.; Angeles-Wedler, D.; Fritsch, D.; Mackenzie, K. Pd-catalyzed hydrodechlorination of chlorinated aromatics in contaminated waters—Effects of surfactants, organic matter and catalyst protection by silicone coating. *Appl. Catal., B* **2010**, *96* (3−4), 323−328.
(27) Paidar, M.; Bouzek, K.; Bergmann, H. Influence of cell construction on the electrochemical reduction of nitrate. *Chem. Eng. J.* **2002**, *85* (2−3), 99−109.
(28) Rivera, F. F.; de León, C. P.; Nava, J. L.; Walsh, F. C. The filter-press FM01-LC laboratory flow reactor and its applications. *Electrochim. Acta* **2015**, *163*, 338−354.
(29) Chen, L.; Shi, J. Chemical-assisted hydrogen electrocatalytic evolution reaction (CAHER). *J. Mater. Chem. A* **2018**, *6* (28), 13538−13548.
(30) Chen, F.-Y.; Wu, Z.-Y.; Gupta, S.; Rivera, D. J.; Lambeets, S. V.; Pecaut, S.; Kim, J. Y. T.; Zhu, P.; Finfrock, Y. Z.; Meira, D. M.; et al. Efficient conversion of low-concentration nitrate sources into ammonia on a Ru-dispersed Cu nanowire electrocatalyst. *Nat. Nanotechnol.* **2022**, *17* (7), 759−767.
(31) Wahlberg, A.; Pettersson, L. J.; Bruce, K.; Andersson, M.; Jansson, K. Preparation, evaluation and characterization of copper catalysts for ethanol fuelled diesel engines. *Appl. Catal., B* **1999**, *23* (4), 271−281.
(32) Sun, G.; Xu, A.; He, Y.; Yang, M.; Du, H.; Sun, C. Ruthenium catalysts supported on high-surface-area zirconia for the catalytic wet oxidation of N, N-dimethyl formamide. *J. Hazard. Mater.* **2008**, *156* (1−3), 335−341.
(33) Shuai, D.; Choe, J. K.; Shapley, J. R.; Werth, C. J. Enhanced activity and selectivity of carbon nanofiber supported Pd catalysts for nitrite reduction. *Environ. Sci. Technol.* **2012**, *46* (5), 2847−2855.
(34) Czioska, S.; Boubnov, A.; Escalera-López, D.; Geppert, J.; Zagalskaya, A.; Röse, P.; Saraçi, E.; Alexandrov, V.; Krewer, U.; Cherevko, S.; et al. Increased Ir-Ir interaction in iridium oxide during the oxygen evolution reaction at high potentials probed by operando spectroscopy. *ACS Catal.* **2021**, *11* (15), 10043−10057.
(35) USEPA. *Work Breakdown Structure-Based Cost Model for Anion Exchange Drinking Water Treatment*; United States Environmental Protection Agency, 2017.


https://doi.org/10.1021/acsestengg.4c00203
*ACS EST Engg.* 2024, 4, 2186−2197

(36) USEPA. *Work Breakdown Structure-Based Cost Model for Granular Activated Carbon Drinking Water Treatment*; United States Environmental Protection Agency, 2021. https://www.epa.gov/sdwa/drinking-water-treatment-technology-unit-cost-models.
(37) USEPA. *Work Breakdown Structure-Based Cost Model for Reverse Osmosis/Nanofiltration Drinking Water Treatment*; United States Environmental Protection Agency, 2021.
(38) Phul, R.; Kaur, C.; Farooq, U.; Ahmad, T. Ascorbic acid assisted synthesis, characterization and catalytic application of copper nanoparticles. *Mater. Sci. Eng. Int. J.* **2018**, *2*, 90−94.
(39) Gopinath, K.; Karthika, V.; Gowri, S.; Senthilkumar, V.; Kumaresan, S.; Arumugam, A. Antibacterial activity of ruthenium nanoparticles synthesized using Gloriosa superba L. leaf extract. *J. Nanostruct. Chem.* **2014**, *4*, 83.
(40) Guerrero-Ortega, L.; Ramírez-Meneses, E.; Cabrera-Sierra, R.; Palacios-Romero, L.; Philippot, K.; Santiago-Ramírez, C. R.; Lartundo-Rojas, L.; Manzo-Robledo, A. Pd and Pd@ PdO core-shell nanoparticles supported on Vulcan carbon XC-72R: comparison of electroactivity for methanol electro-oxidation reaction. *J. Mater. Sci.* **2019**, *54* (21), 13694−13714.
(41) Vinokurov, K.; Bekenstein, Y.; Gutkin, V.; Popov, I.; Millo, O.; Banin, U. Rhodium growth on Cu 2 S nanocrystals yielding hybrid nanoscale inorganic cages and their synergistic properties. *CrystEngComm* **2014**, *16* (40), 9506−9512.
(42) Biesinger, M. C. Advanced analysis of copper X-ray photoelectron spectra. *Surf. Interface Anal.* **2017**, *49* (13), 1325−1334.
(43) Yang, Y.; Yu, Y.; Li, J.; Chen, Q.; Du, Y.; Rao, P.; Li, R.; Jia, C.; Kang, Z.; Deng, P.; et al. Engineering ruthenium-based electrocatalysts for effective hydrogen evolution reaction. *Nano-Micro Lett.* **2021**, *13*, 160.
(44) Bridier, B.; López, N.; Pérez-Ramírez, J. Partial hydrogenation of propyne over copper-based catalysts and comparison with nickel-based analogues. *J. Catal.* **2010**, *269* (1), 80−92.
(45) Qu, J.; Zou, X.; Liu, B.; Dong, S. Assembly of polyoxometalates on carbon nanotubes paste electrode and its catalytic behaviors. *Anal. Chim. Acta* **2007**, *599* (1), 51−57.
(46) Bard, A. J.; Faulkner, L. R.; White, H. S. *Electrochemical Methods: Fundamentals and Applications*; John Wiley & Sons, 2022.
(47) Mao, R.; Zhao, X.; Lan, H.; Liu, H.; Qu, J. Graphene-modified Pd/C cathode and Pd/GAC particles for enhanced electrocatalytic removal of bromate in a continuous three-dimensional electrochemical reactor. *Water Res.* **2015**, *77*, 1−12.
(48) Xiao, W.; Liutheviciene Cordeiro, M. A.; Gong, M.; Han, L.; Wang, J.; Bian, C.; Zhu, J.; Xin, H. L.; Wang, D. Optimizing the ORR activity of Pd based nanocatalysts by tuning their strain and particle size. *J. Mater. Chem. A* **2017**, *5* (20), 9867−9872.
(49) Cao, X. T.; Kabtamu, D. M.; Kumar, S.; Varma, R. S. Advances in Thermo-Photo-and Electrocatalytic Continuous Conversion of Carbon Dioxide into Liquid Chemicals. *ACS Sustainable Chem. Eng.* **2022**, *10* (39), 12906−12932.
(50) Kim, H. J.; Lee, J.; Green, S. K.; Huber, G. W.; Kim, W. B. Selective glycerol oxidation by electrocatalytic dehydrogenation. *ChemSusChem* **2014**, *7* (4), 1051−1056.
(51) Alebrahim, M. F.; Khattab, I.; Sharif, A. O. Electrodeposition of copper from a copper sulfate solution using a packed-bed continuous-recirculation flow reactor at high applied electric current. *Egypt. J. Pet.* **2015**, *24* (3), 325−331.
(52) Troutman, J. P.; Li, H.; Haddix, A. M.; Kienzle, B. A.; Henkelman, G.; Humphrey, S. M.; Werth, C. J. PdAg alloy nanocatalysts: toward economically viable nitrite reduction in drinking water. *ACS Catal.* **2020**, *10* (14), 7979−7989.
(53) Wang, L.; Lavacchi, A.; Bellini, M.; D'Acapito, F.; Benedetto, F. D.; Innocenti, M.; Miller, H. A.; Montegrossi, G.; Zafferoni, C.; Vizza, F. Deactivation of palladium electrocatalysts for alcohols oxidation in basic electrolytes. *Electrochim. Acta* **2015**, *177*, 100−106.
(54) Palomares, A. E.; Franch, C.; Corma, A. Nitrates removal from polluted aquifers using (Sn or Cu)/Pd catalysts in a continuous reactor. *Catal. Today* **2010**, *149* (3−4), 348−351.
(55) Yan, C.; Lee, K.-L.; Troutman, J. P.; Brady, C. E.; Humphrey, S. M.; Cwiertny, D. M.; Mubeen, S.; Werth, C. J. Tailored Copper-Based Cathode Design Advances Economic Viability of Electrocatalytic Nitrate Treatment with Ammonia Recovery in a Scalable Flow Reactor. *Appl. Catal., B* **2024**, *357*, 124278.
(56) Hashiba, H.; Weng, L.-C.; Chen, Y.; Sato, H. K.; Yotsuhashi, S.; Xiang, C.; Weber, A. Z. Effects of electrolyte buffer capacity on surface reactant species and the reaction rate of CO2 in Electrochemical CO2 reduction. *J. Phys. Chem. C* **2018**, *122* (7), 3719−3726.
(57) Garsany, Y.; Baturina, O. A.; Swider-Lyons, K. E. Impact of sulfur dioxide on the oxygen reduction reaction at Pt/Vulcan carbon electrocatalysts. *J. Electrochem. Soc.* **2007**, *154* (7), B670.
(58) König, M.; Vaes, J.; Klemm, E.; Pant, D. Solvents and supporting electrolytes in the electrocatalytic reduction of CO2. *Iscience* **2019**, *19*, 135−160.
(59) Kishimoto, N.; Matsuda, N. Bromate ion removal by electrochemical reduction using an activated carbon felt electrode. *Environ. Sci. Technol.* **2009**, *43* (6), 2054−2059.
(60) McPherson, I. J.; Ash, P. A.; Jones, L.; Varambhia, A.; Jacobs, R. M.; Vincent, K. A. Electrochemical CO oxidation at platinum on carbon studied through analysis of anomalous in situ IR spectra. *J. Phys. Chem. C* **2017**, *121* (32), 17176−17187.
(61) He, L.; Zeng, T.; Yao, F.; Zhong, Y.; Tan, C.; Pi, Z.; Hou, K.; Chen, S.; Li, X.; Yang, Q. Electrocatalytic reduction of nitrate by carbon encapsulated Cu-Fe electroactive nanocatalysts on Ni foam. *J. Colloid Interface Sci.* **2023**, *634*, 440−449.
(62) He, L.; Yao, F.; Zhong, Y.; Tan, C.; Hou, K.; Pi, Z.; Chen, S.; Li, X.; Yang, Q. Achieving high-performance electrocatalytic reduction of nitrate by N-rich carbon-encapsulated Ni-Cu bimetallic nanoparticles supported nickel foam electrode. *J. Hazard. Mater.* **2022**, *436*, 129253.
(63) Yao, F.; Jia, M.; Yang, Q.; Chen, F.; Zhong, Y.; Chen, S.; He, L.; Pi, Z.; Hou, K.; Wang, D.; et al. Highly selective electrochemical nitrate reduction using copper phosphide self-supported copper foam electrode: Performance, mechanism, and application. *Water Res.* **2021**, *193*, 116881.
(64) Xu, Z.; Han, D.; Li, Y.; Zhang, P.; You, L.; Zhao, Z. High removal performance of a magnetic FPA90-Cl anion resin for bromate and coexisting precursors: kinetics, thermodynamics, and equilibrium studies. *Environ. Sci. Pollut. Res.* **2018**, *25*, 18001−18014.
(65) Yan, H.; Du, X.; Li, P.; Yu, S.; Tang, Y. Adsorption of bromate from aqueous solutions by modified granular activated carbon: Batch and column tests. *Ozone: Sci. Eng.* **2015**, *37* (4), 357−370.
(66) Singh, N.; Goldsmith, B. R. Role of electrocatalysis in the remediation of water pollutants. *ACS Catal.* **2020**, *10* (5), 3365−3371.
(67) Krishnan, S.; Koning, V.; Theodorus de Groot, M.; de Groot, A.; Mendoza, P. G.; Junginger, M.; Kramer, G. J. Present and future cost of alkaline and PEM electrolyser stacks. *Int. J. Hydrogen Energy* **2023**, *48*, 32313−32330.


https://doi.org/10.1021/acsestengg.4c00203
*ACS EST Engg.* 2024, 4, 2186−2197